Electronic Supplementary Material (ESI) for Environmental Science: Nano.

Supplementary Information

The Influence of Surface Coating Functionality on the Aging of Nanoparticles in Wastewater

Mark C. Surette[1,2], Jeffrey A. Nason[1], and Ralf Kaegi[2]

[1] School of Chemical, Biological and Environmental Engineering
Oregon State University, 116 Johnson Hall, Corvallis, Oregon 97331, United States

[2] Eawag, Swiss Federal Institute of Aquatic Science and Technology
Überlandstrasse 133, CH-8600 Dübendorf, Switzerland

32 Pages

4 Tables

24 Figures

Characterization of Pristine Model Engineered Nanoparticles

The manufacturer reported specifications and measured characteristics of the model engineered nanomaterials (ENMs) are provided in Table 1 (main text). The values were determined as follows:

- **Core Diameter (D_c):** Manufacturer reported specification. Measured via transmission electron microscopy (TEM) using a JEM-1010 TEM (JEOL).
- **Intensity-weighted hydrodynamic diameter ($D_{h,initial}$):** Measured via dynamic light scattering (DLS) at 1 mg Au/L in 0.02 µm filtered 18.2 MΩ-cm Nanopure water (DDI; Barnstead) using a ZetaSizer Nano ZS (Malvern Panalytical). Each replicate measurement (n = 34) was performed for 1-minute.
- **Electrophoretic mobility (μ_E):** Measured at 5 mg Au/L in pH-adjusted (pH 5.3 – 5.6) 1 mM NaCl (prepared in 0.02 µm filtered DDI) using a Folded Capillary Zeta Cell with a ZetaSizer Nano ZS (Malvern Panalytical). Each replicate measurement (n = 9) was performed for 30 cycles. Details on the conversion of the measured EPM to modelled zeta potential (ζ) are provided in the next section.
- **Surface Plasmon Resonance (λ_{SPR}):** Measured via ultraviolet-visible light spectroscopy (UV-Vis) at 5 mg Au/L in 0.02 µm filtered DDI using a Cary-60 UV-Vis (Agilent Technologies). Each replicate measurement (n = 3) was performed at λ = 400 – 800 nm at a scan rate of 2 nm/s using a 10 mm light-path Quartz Suprasil® micro-cuvette (Hellma Analytics).

Zeta Potential Calculation in Simple Electrolyte Solution (1 mM NaCl)

The measured EPM (μ_E), reported in Table 1 (main text), were converted to zeta potential (ζ) according to Henry (1931) with the correction $f_1(\kappa a)$ applied according to Ohshima (1994), resulting in the following equation:

$$\zeta = \frac{3\mu_E\eta}{2\epsilon_w f_1(\kappa a)} = \frac{3\mu_E\eta}{2\epsilon_w\left(1+\frac{1}{2\left[1+\frac{\delta}{\kappa a}\right]^3}\right)} \quad (1)$$

Where:

$$\delta = \frac{2.5}{1+2e^{-\kappa a}} \quad (2)$$

The definition of the variables in Equations 1 and 2, along with their corresponding values, are shown in Table S1.

Table S1. Inputs used to calculate ζ from μ_E.

Input	Value[a]	Source
Permittivity in Water (ϵ_w)	6.95 $x10^{-10}$ C^2/J-m	Known – H_2O
Medium Dynamic Viscosity (η)	1 $x10^{-3}$ N-s/m^2	Known – H_2O
Ohshima Fitting Parameter (δ)	2 – 2.04	Calculated per Hunter (2001)
Debye Length (κ)	0.104 nm^{-1}	Calculated per Benjamin & Lawler (2013)
Particle Radius (a)	20 – 21 nm	Measured (Table 1)

[a] All values at 25 °C.

Removal of Gold Nanoparticles in Unaltered Wastewater Matrices

The removal of the gold nanoparticles (AuNPs) via heteroaggregation with the suspended particulate matter (SPM) in all three unaltered wastewater matrix was verified. Batch experiments were performed by dosing samples (V_{TOT} = 75 mL) of each unaltered wastewater matrix to C_{NP} = 1 mg Au/L. Upon dosing, each batch was continuously mixed for ≈45 minutes (comparable to the measurement period of the time resolved dynamic light scattering [TR-DLS] experiments), after which the mixing was stopped and a settling period of ≈30 minutes was used to remove the bulk of the SPM and any associated ENMs. Then, 15 mL of the supernatant was removed and digested using a combination of H_2O_2 (to remove organics) and fresh *aqua regia* (3:1 ultrapure HCl:HNO_3; to dissolve AuNPs) via microwave digestion. Triplicate samples of the digestate were prepared and analyzed via inductively-coupled plasmas mass spectroscopy (ICP-MS) using a 7500-CE ICP-MS (Agilent Technologies, Inc.) to quantify the concentration of AuNPs remaining in suspension (Figure S1).

Significantly less removal was noted in the influent wastewater matrix relative to that measured in the denitrification and nitrification matrices. This likely reflects the lower number concentration of suspended solids in the influent wastewater compared to the biological treatment stages where suspended solids are both concentrated and created during biological growth. The increased concentration of suspended solids would increase both the aggregation rate and the total surface area for the AuNPs to attach to.

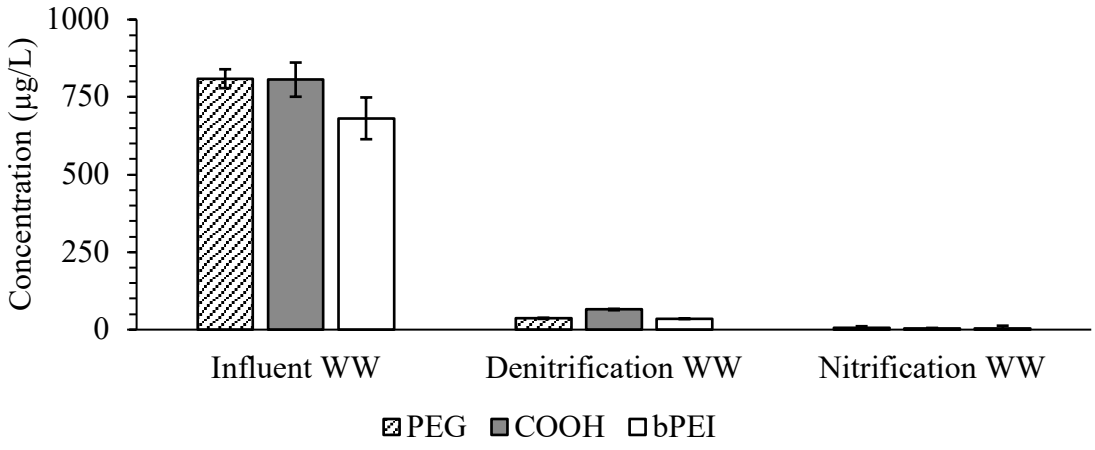

Figure S1: Concentration of each AuNP remaining in suspension in unaltered wastewater matrices after ≈ 45 minutes. Error bars indicate ± 95% confidence interval (n = 3 – 5).

Properties of Wastewater Matrices

The aquatic chemistry of the influent, denitrification, and nitrification wastewater matrices was measured by collecting a 1L sample from the primary clarifier and activated sludge treatment stage (anoxic and aerobic tanks), respectively, between 9:00-10:00 a.m. The samples were immediately centrifuged at 3,000 rpm (≈1,860*g* RCF) for 30 minutes and the supernatant (≈900 mL) was sequentially filtered through 1 µm and 0.45 µm cellulose-acetate filters using a stainless steel pressure filtration unit (Sartorius). The filtered samples were then analyzed according to the methods described in the American Water Works Association (AWWA) *Standard Methods for the Examination of Water and Wastewater, 22nd Edition* (American Public Health Association, 2012). The results are summarized in Table S2.

Table S2. Characteristics of 0.45 µm-filtered wastewater matrices.

	Influent	Denitrification (Anoxic)	Nitrification (Aerobic)
Conductivity (µS/cm)	1,358	1,182	1,151
Ionic Strength (mM)[a]	21.7	18.9	18.4
pH	8.16	7.65	7.76
Dissolved Organic Carbon (mg/L)[b]	168.0	16.4	45.9
Inorganic Non-Metallic Constituents[c]			
NH_4^+ (mg/L as N)	17.3	2.1	16.3
NO_2^- (mg/L as N)	0.25	0.58	0.5
NO_3^- (mg/L as N)	1.4	9.2	<0.2
PO_4^{3-} (mg/L as P)	2.5	1.3	1.2
Metals[d]			
Ca^{2+} (mg/L)	94.4	87.8	84.2
Mg^{2+} (mg/L)	10.7	11.2	10.4
K^+ (mg/L)	65.3	78.1	68.7
Na^+ (mg/L)	185.6	195.6	193.3

[a] Calculated using $I = 1.6 \times 10^{-5} \times$ S.C.
[b] Measured via Method 5310-B.
[c] Measured via Method 4110.
[d] Measured via Method 3120.

Data Treatment of UV-Vis Spectra – Batch Experiments

For each UV-Vis measurement, the background-corrected UV-Vis spectrum was generated by subtracting the blank-corrected background spectrum (measured prior to the addition of the AuNPs) from the UV-Vis spectrum measured at each 20-minute interval after the addition of the AuNPs (Figure S2a-b). The background-corrected and normalized (A/A_{max}) UV-Vis spectrum was generated by dividing the background-corrected absorbance at each wavelength (A) by the maximum absorbance (A_{max}) that was measured (Figure S2c-d).

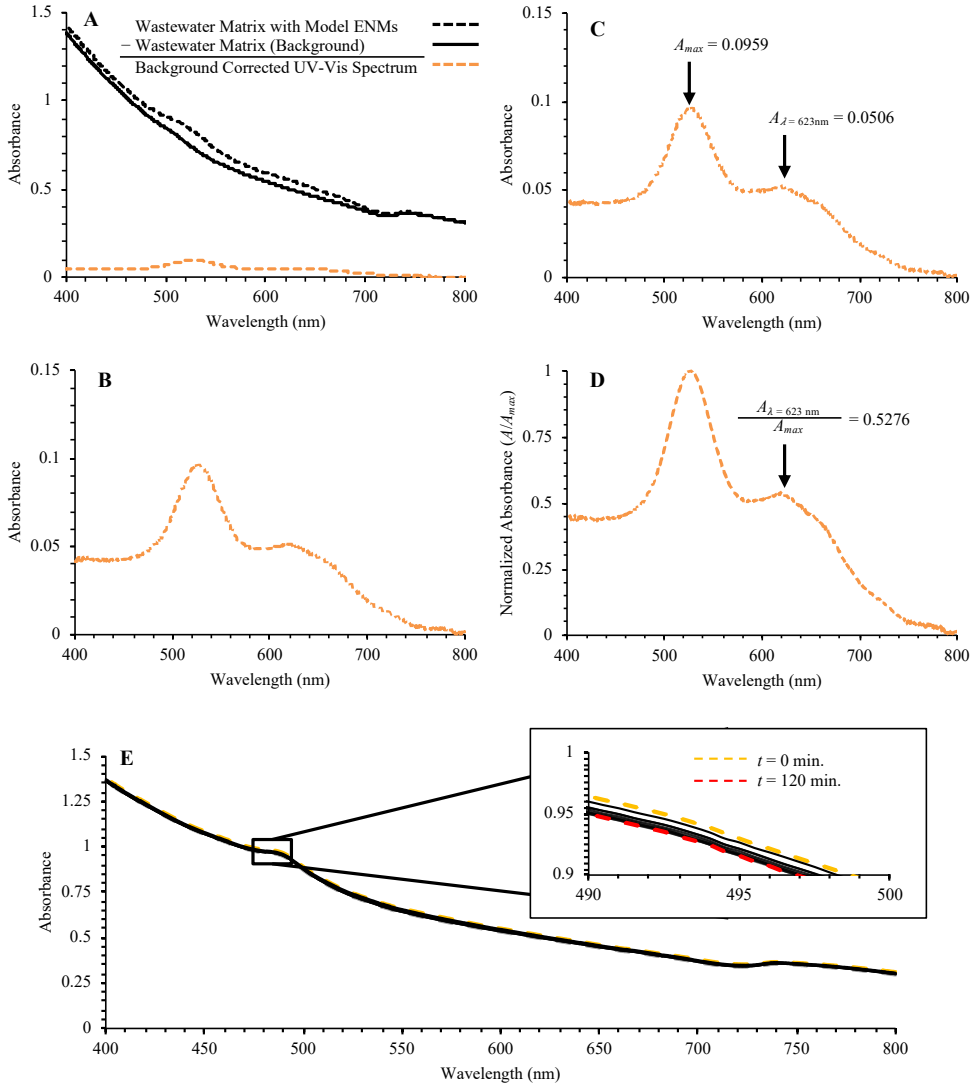

Figure S2. Illustrative example of UV-Vis data treatment steps, shown for PEG-AuNPs in influent wastewater matrix. (a) generation of background-corrected UV-Vis spectrum, (b) enlargement of background-corrected UV-Vis spectrum, (c) identification of λ_{max}, (d) generation of background-corrected and normalized UV-Vis spectrum, and (e) variation in background UV-Vis spectra (influent wastewater matrix).

Matrix Exchange using Tangential-Flow Filtration System

To perform the matrix exchange experiments, a tangential-flow filtration (TFF) system was used. A process flow diagram for the system is shown in Figure S3. Note that during the baseline testing, only the influent wastewater matrix was added to the TFF reservoir. We chose to simultaneously add the denitrification and nitrification wastewater matrices from $t = 40 – 140$ minutes rather than adding them one at a time. Two other alternative approaches were considered, both operating the TFF system like a sequencing batch reactor. The first was to significantly reduce the amount of a given wastewater matrix before adding the next matrix, without continuously drawing and analyzing samples (i.e., $F_R = 0$ mL/minute). This approach would require a significant amount of time for each matrix exchange step (≈18 hours to remove ≈90% of V_{TOT} via F_P alone) while simultaneously increasing the AuNP concentration in the retentate, thus introducing artifacts that would complicate our analysis. The second approach was to operate the system in a similar manner (i.e., reduce V_{TOT} by ≈90%) but continuously withdraw and analyze samples. This approach would hinder analysis of the AuNPs after exposure to the denitrification and nitrification wastewater matrices, since the concentration of AuNPs in the TFF system would have been significantly reduced, via withdrawal in F_P, prior to the introduction of the additional matrices. While not exactly mimicking the processes occurring in a full-scale WWTP, our approach is considered a compromise and was intended to serve as a proxy for the transport processes occurring in a WWTP while enabling an investigation of ENM transformations exposed to changing wastewater matrices.

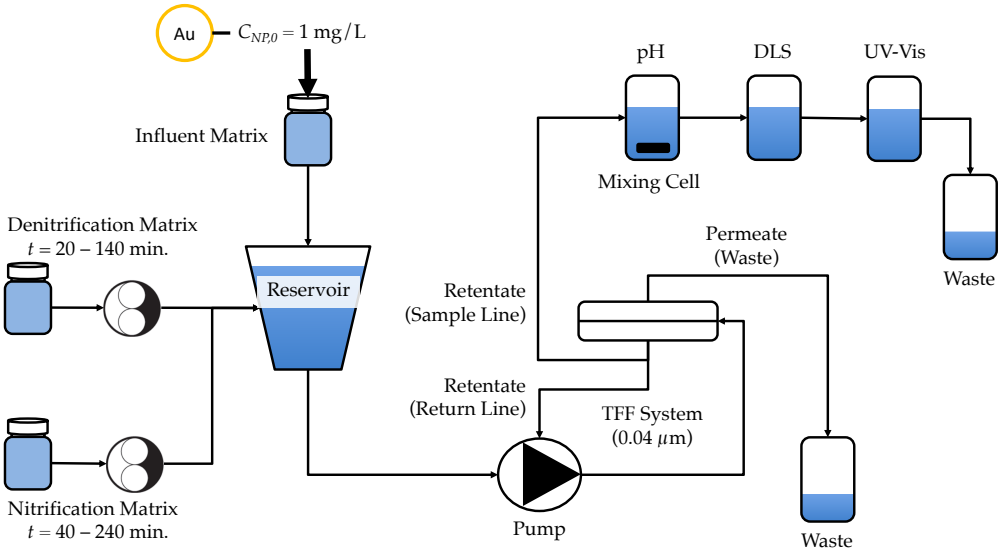

Figure S3. Process flow diagram for TFF system coupled with in-line DLS and UV-Vis detectors.

Figure S4 shows the results of modelling to estimate the volume fraction of each wastewater matrix within the TFF system during the double matrix exchange process, assuming complete mixing. After the initial period when only the influent wastewater matrix is present, the fraction of the denitrification wastewater matrix in the TFF system steadily increases, reaching a maximum of ≈25% at t = 140 min., at which point the addition of the denitrification wastewater matrix was stopped. The fraction of the nitrification wastewater also steadily increases after t = 40 min., reaching a maximum of ≈50% at t = 240 min., at which point the procedure was stopped.

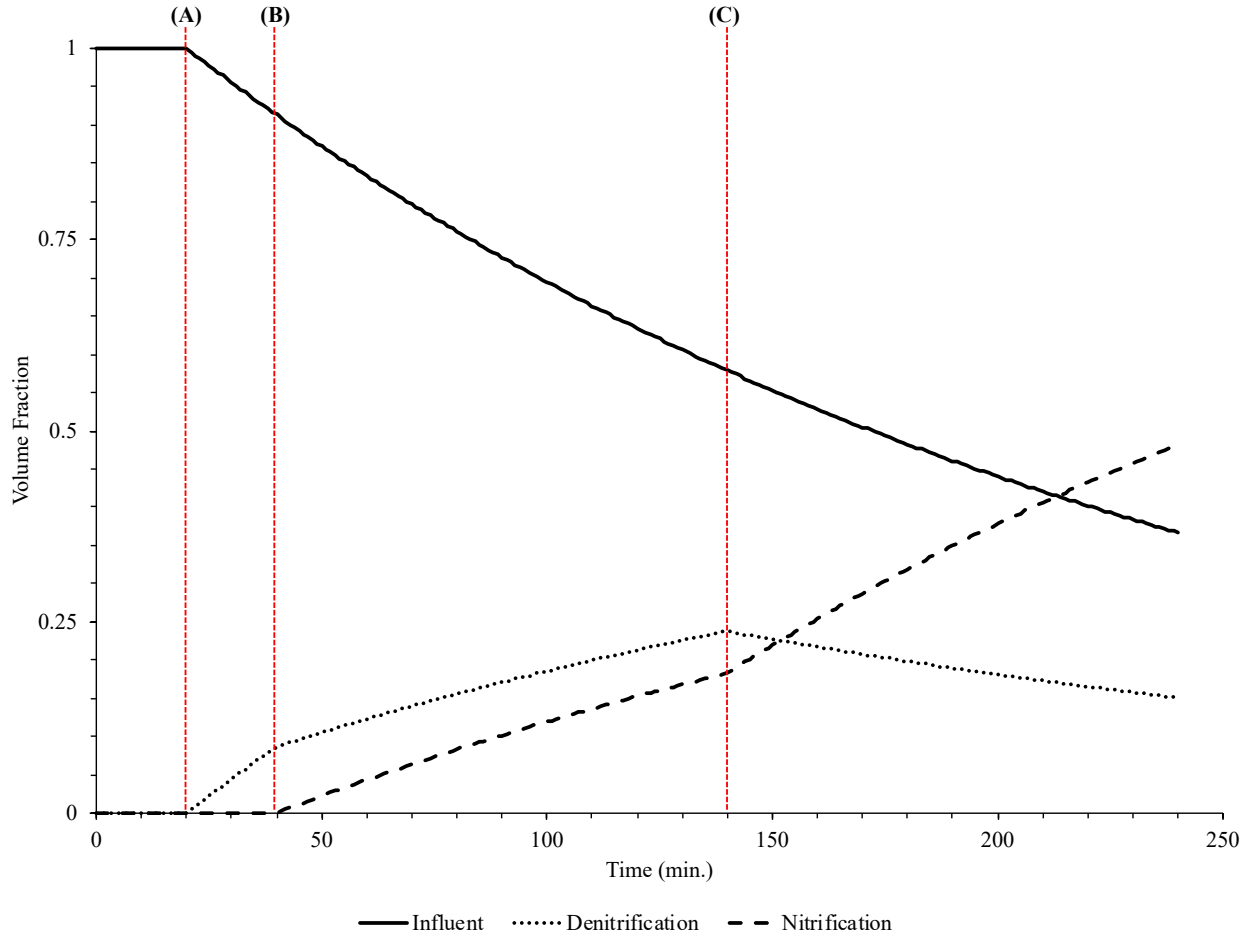

Figure S4. Estimated volume fraction of each wastewater matrix in the TFF system during the double matrix exchange. (a) Commencement of denitrification matrix addition, (b) commencement of nitrification matrix addition, and (c) cessation of denitrification matrix addition while continuing addition of nitrification matrix.

Testing of Tangential-Flow Filtration System

The ability of the TFF membrane to retain the AuNPs was tested by the following procedure:

1. A 300 mL sample containing the AuNPs was prepared by dispersing the bPEI-AuNPs in 0.02 μm filtered 18.2 MΩ-cm Nanopure water (DDI; Barnstead) to C_{NP} = 0.5 mg/L (V_{DDI} = 297 mL; V_{AuNP} = 3 mL).
2. Upon preparation of the sample, aliquots were collected in triplicate (V_{TOT} = 10 mL) via calibrated pipette and transferred to separate 15 mL polypropylene tubes to confirm the initial solution concentration. The remainder of the sample was transferred to the TFF reservoir.
3. The TFF system was then operated at a transmembrane pressure (TMP) of 2-3 bar, a cross-flow velocity (V_s) of ≈1.4 cm/s, and at T = 19 – 20 °C, with a 0.04 μm PES membrane installed in the filter housing.
4. The AuNP/DDI matrix was cycled through the TFF system until sufficient volume (≥ 30 mL) had been obtained in the permeate vessel.
5. The permeate vessel was briefly mixed via gentle shaking and aliquots were collected in triplicate (V_{TOT} = 10 mL) via calibrated pipette and transferred to separate 15 mL polypropylene tubes.
6. The samples were then microwave digested in fresh *aqua regia* (3:1 HCl:HNO_3) and analyzed via inductively coupled plasma mass spectrometry (ICP-MS).

The results, shown in Table S3, indicate that ≈99% of the AuNP mass was retained within the TFF system.

Table S3. Concentration of bPEI-AuNPs in TFF permeate.

	Average Concentration (μg/L)
Initial Solution	525.73 ± 166.9
Permeate	5.50 ± 1.0

Error bars indicate ± 95% confidence interval (n = 3).

Data Treatment of UV-Vis Spectra – Matrix Exchange

The TR-UV-Vis spectra measured during the matrix exchange procedure were generated following the same overall steps as the batch experiments. Unlike the batch experiments, the background UV-Vis spectra were found to change over time before stabilizing (Figure S5a). This likely reflects an initial change in the composition of the background wastewater matrix as some constituents, such as small organic macromolecules, are selectively removed via filtration through the PES membrane (0.04 μm) of the tangential flow filtration (TFF) system.

To address this, the background spectra was measured over time by operating the TFF system with only with the background matrix (or matrices, in the case of the double matrix exchange) and measuring the UV-Vis spectrum at 5-minute intervals (Figure S5a). The experiment then proceeded as described in the main text, generating the uncorrected UV-Vis spectra for a given AuNP type and wastewater matrix combination. The background-corrected UV-Vis spectra (Figure S5b) were then generated by subtracting the previously measured background spectra (Figure S5a) from the corresponding uncorrected UV-Vis spectra measured at each interval. To account for negative absorbance values, attributed to the 'blanking' of the instrument with 18.2 MΩ-cm Nanopure water (DDI; Barnstead) between each experiment, a correction of 0.3 A.U. was applied to all the background-corrected UV-Vis spectra at each wavelength and time interval. Because our analysis focuses on the relative locations and heights of peaks, this offset does not affect the resulting conclusions. The background-corrected and normalized (A/A_{max}) UV-Vis spectra were generated by dividing the background-corrected absorbance at each wavelength (A) by the maximum absorbance (A_{max}) that was measured (Figure S5c). A moving average window (n = 15) was then applied to smooth the data (Figure S5d).

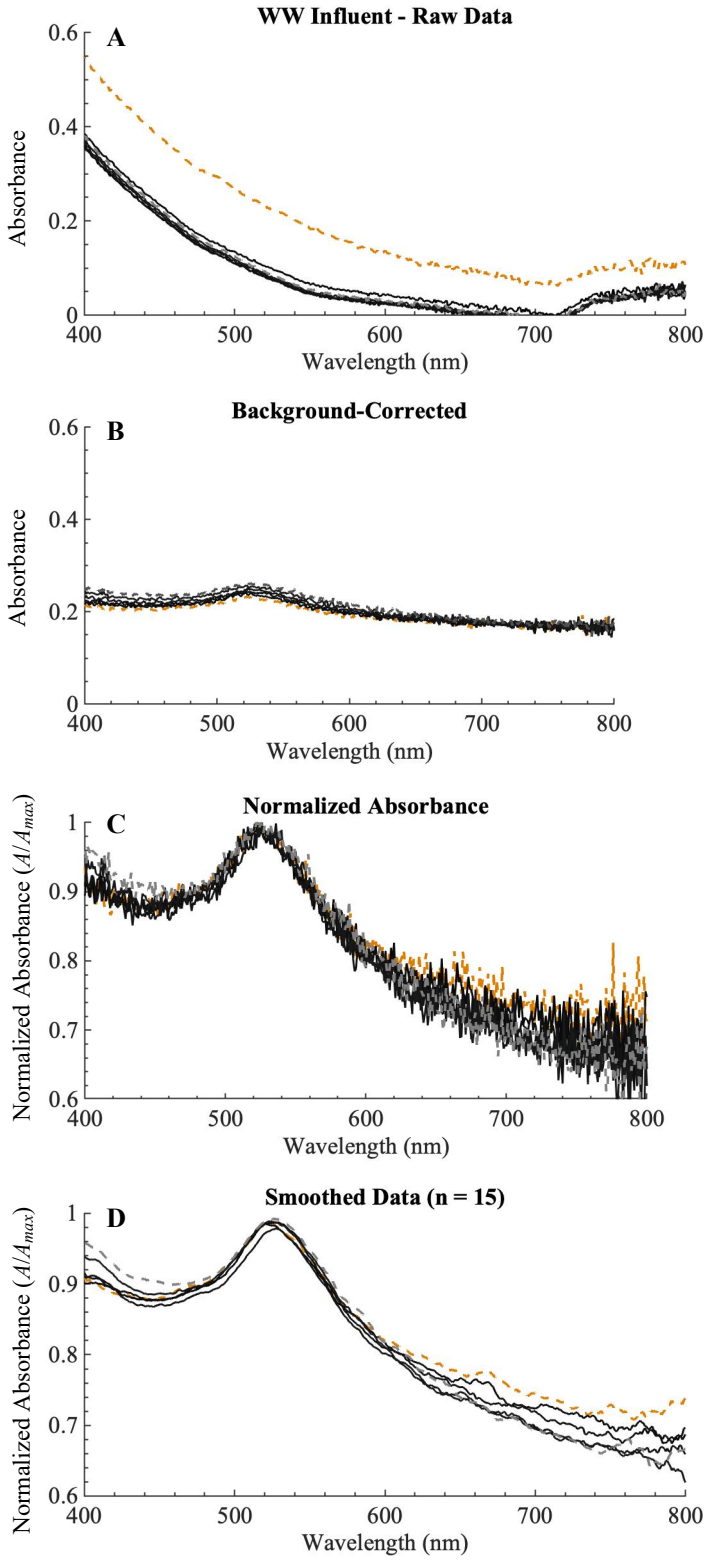

Figure S5. Illustrative example of UV-Vis data treatment steps during matrix exchange procedure, shown for bPEI-AuNPs in influent wastewater matrix (baseline): (a) background wastewater matrix UV-Vis spectra, (b) background-corrected UV-Vis spectra, (c) background-corrected and normalized (A/A_{max}) UV-Vis spectra, and (d) background-corrected, normalized, and smoothed UV-Vis spectra.

Time-Resolved Dynamic Light Scattering

The colloidal stability of each AuNP type upon dispersion in the wastewater matrices was tracked using time-resolved dynamic light scattering (TR-DLS). The samples were prepared and analyzed according to the procedures discussed in the main text. Each AuNP type was measured in each wastewater matrix in triplicate. The results are presented in Figures S6 – S8. In addition, a "long-term" TR-DLS measurement (herein referred to as LT-TR-DLS) was performed to extend the measurement period to ≈120 minutes. During the LT-TR-DLS, the same procedure as that outlined for the TR-DLS measurements was followed, except that a 45-second delay occurred between each of the measurements. The results of the LT-TR-DLS are presented in Figure S9.

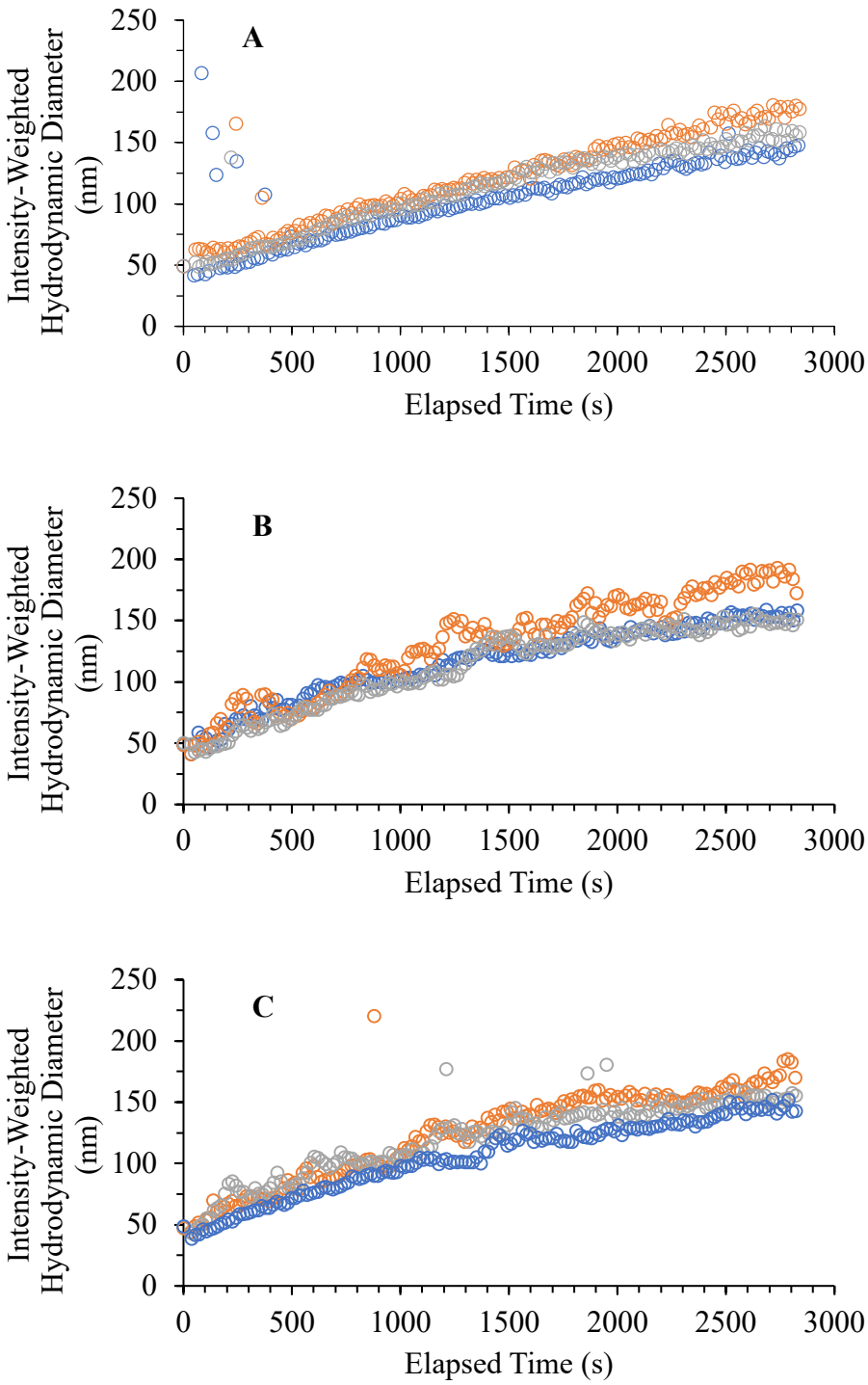

Figure S6: Intensity-weighted hydrodynamic diameter (D_h) over time for PEG-AuNPs in (a) influent, (b) denitrification, and (c) nitrification wastewater matrices.

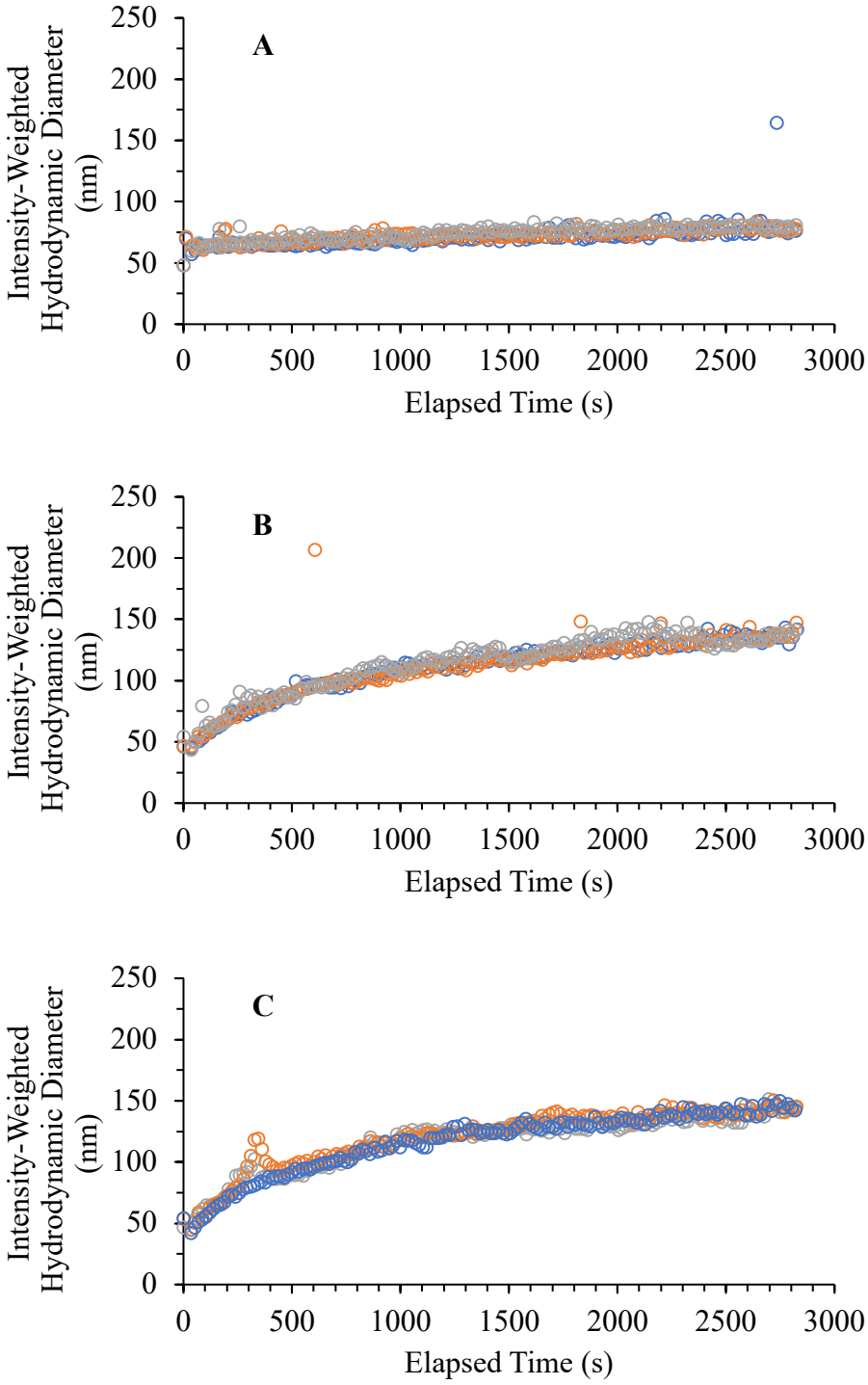

Figure S7: Intensity-weighted hydrodynamic diameter (D_h) over time for COOH-AuNPs in (a) influent, (b) denitrification, and (c) nitrification wastewater matrices.

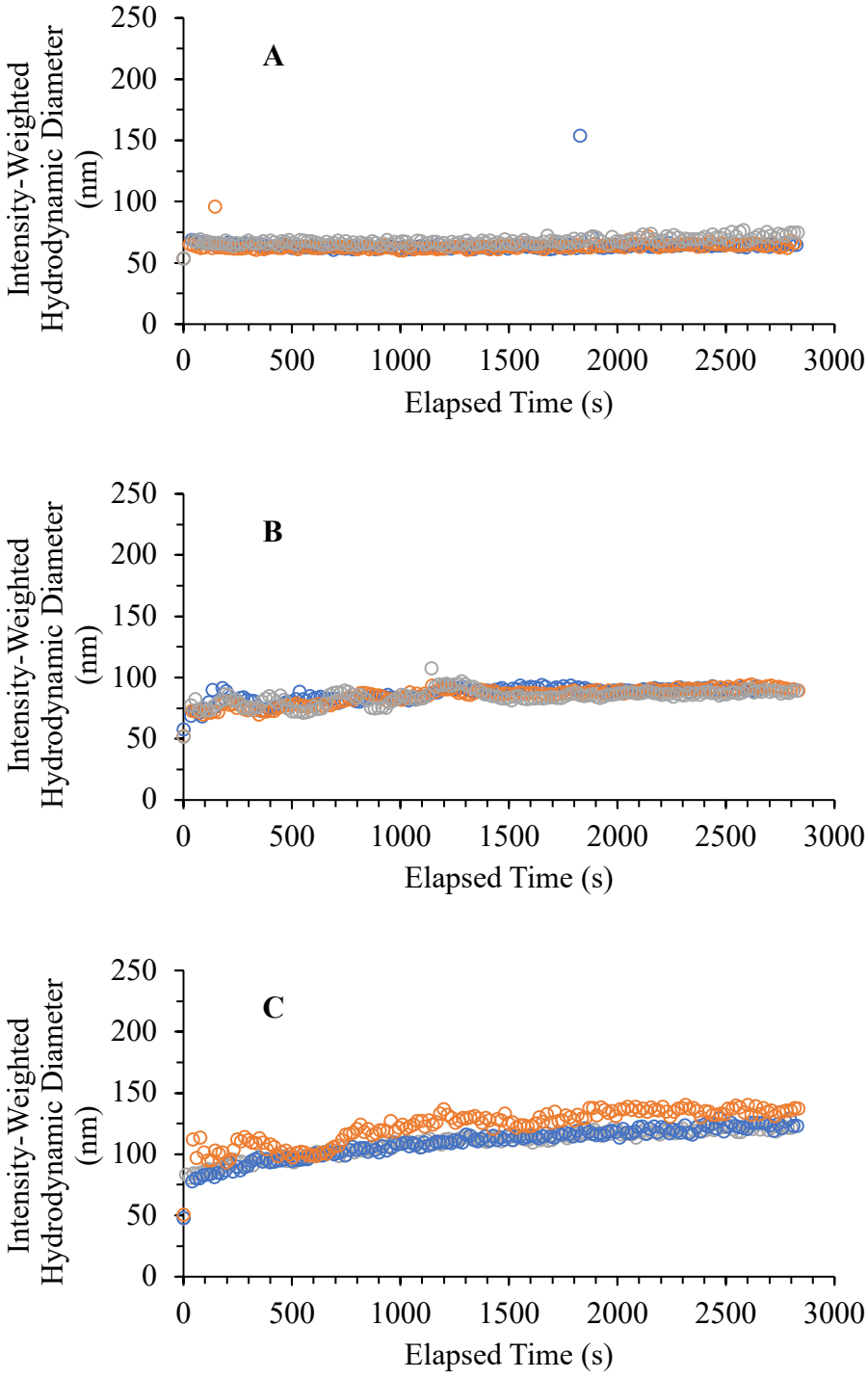

Figure S8: Intensity-weighted hydrodynamic diameter (D_h) over time for bPEI-AuNPs in (a) influent, (b) denitrification, and (c) nitrification wastewater matrices.

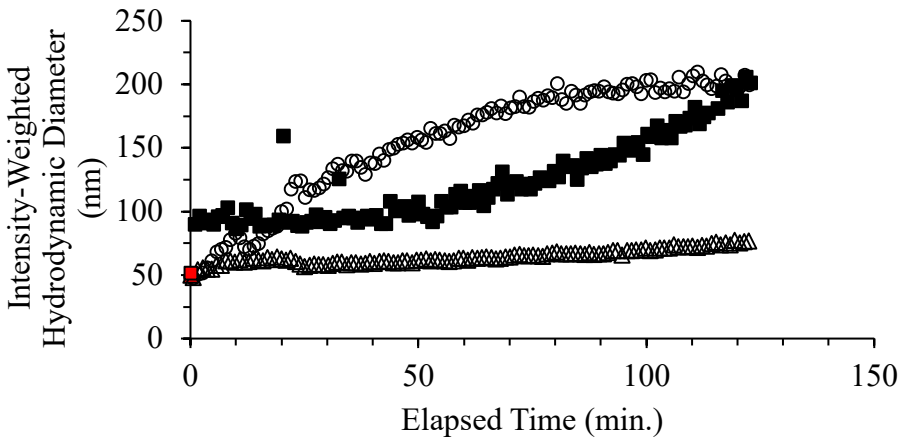

Figure S9: Intensity-weighted hydrodynamic diameter (D_h) over time for (○) PEG-AuNPs, (△) COOH-AuNPs, and (■) bPEI-AuNPs in influent wastewater matrix. $D_{h,initial}$ for each AuNP type shown in red.

Time-Resolved UV-Vis Spectra – Batch Experiments

Conformational changes of the engineered surface coating and/or adsorption of organic macromolecules to the AuNPs, as well as estimates of the AuNP interparticle separation distance, were assessed using time-resolved ultraviolet-visible light spectroscopy (TR-UV-Vis). The samples were prepared and analyzed according to the procedures discussed in the main text. Each AuNP type was measured in each wastewater matrix in triplicate. The replicate measurements are presented in Figures S11 – S19. From these replicate UV-Vis spectra, the red-shift of the primary peak in proximity to λ_{SPR} (Table 1), referred to herein as λ_{max}, was calculated for each AuNP type in each wastewater matrix (Figure S10).

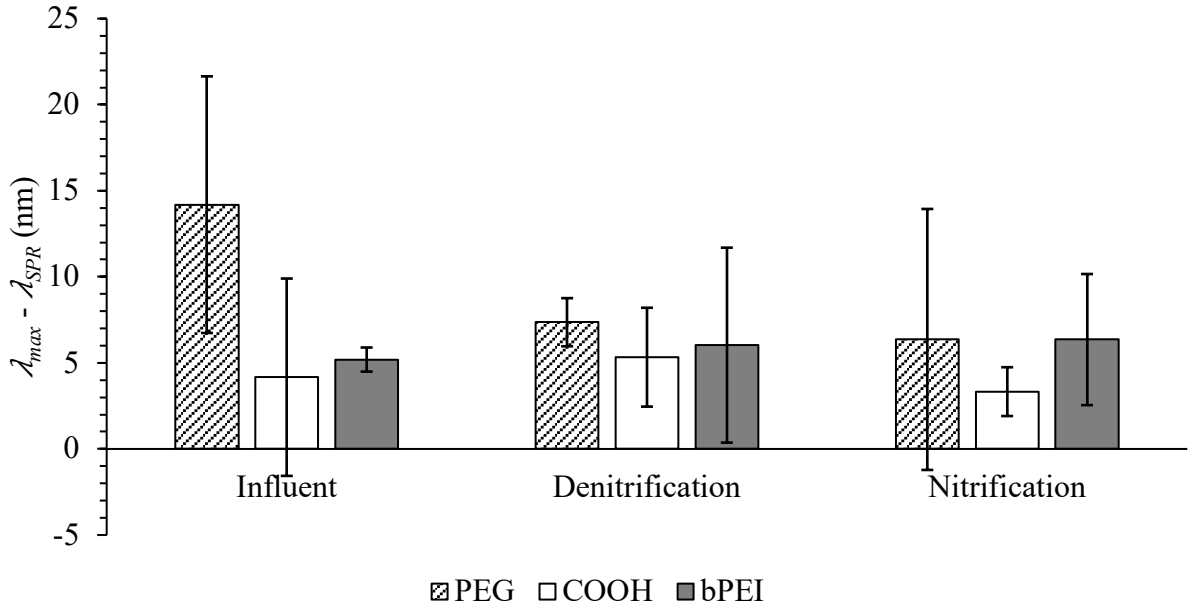

Figure S10. Average red-shift of the primary peak (λ_{max}) in relation to λ_{SPR} for each AuNP type after incubating for 120 minutes in each wastewater matrix. Error bars indicate ± 95% confidence interval (n = 3).

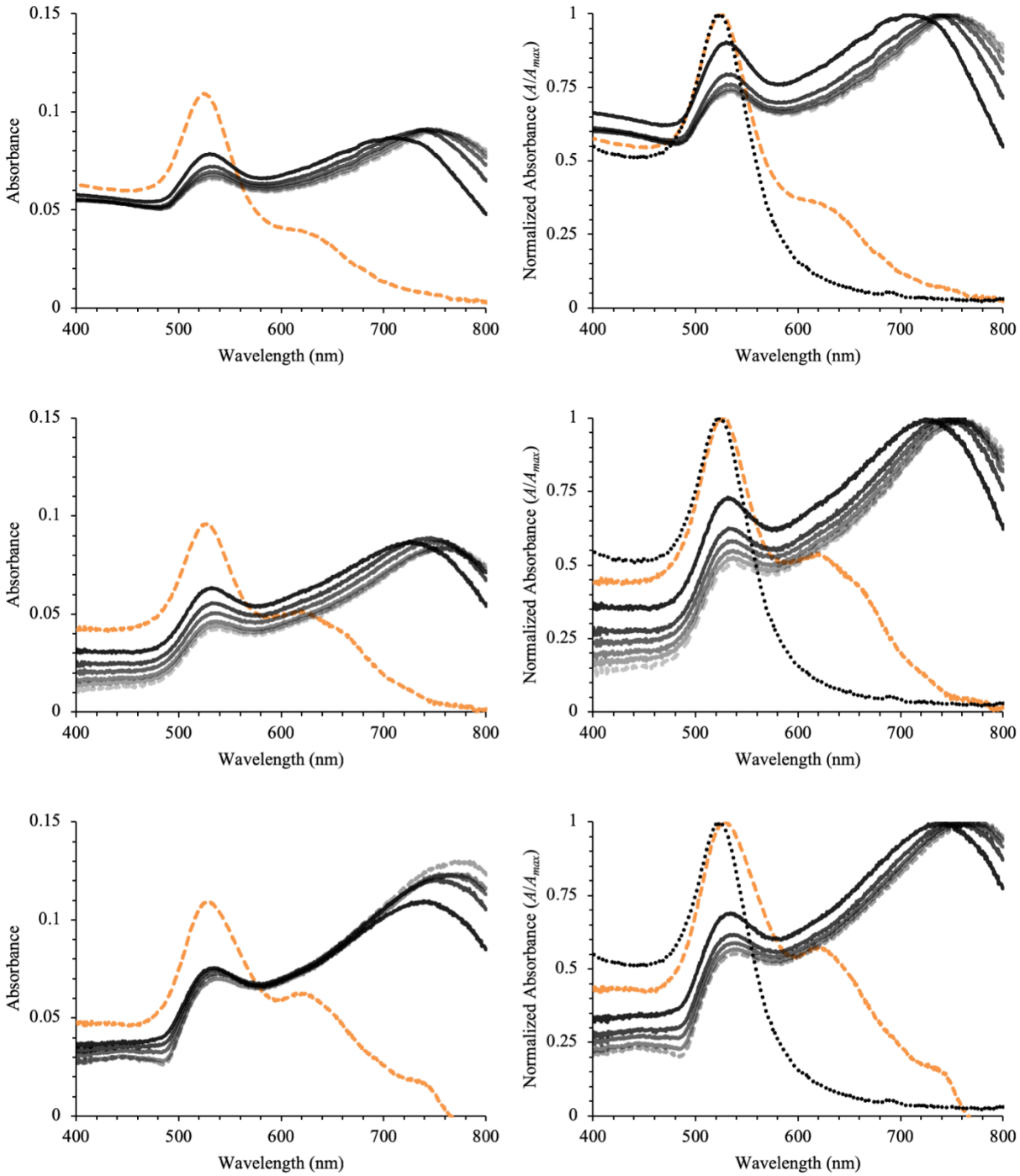

Figure S11. (Left) Background-corrected and (right) background-corrected and normalized (A/A_{max}) UV-Vis spectra for PEG-AuNPs in influent wastewater matrix. Orange dashed-line depicts UV-Vis spectra at $t \approx 0$ minutes, grey dashed-line depicts spectra at $t = 120$ minutes, and grey-scale depicts spectra at 20-minutes intervals in between (black-to-grey). For reference, the black dotted-line depicts the UV-Vis spectra in DDI.

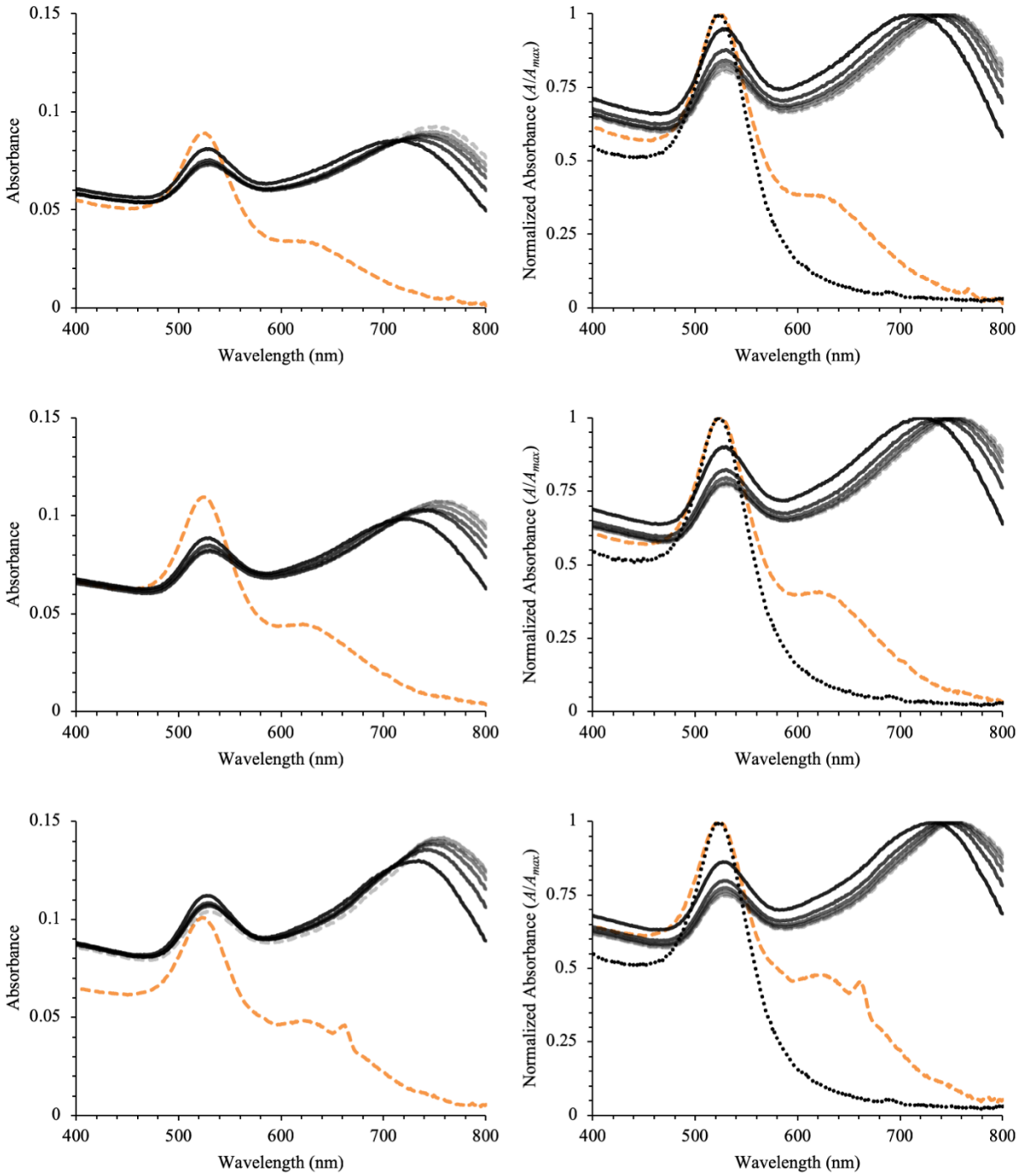

Figure S12. (Left) Background-corrected and (right) background-corrected and normalized (A/A_{max}) UV-Vis spectra for PEG-AuNPs in denitrification wastewater matrix. Orange dashed-line depicts UV-Vis spectra at $t \approx 0$ minutes, grey dashed-line depicts spectra at $t = 120$ minutes, and grey-scale depicts spectra at 20-minutes intervals in between (black-to-grey). For reference, the black dotted-line depicts the UV-Vis spectra in DDI.

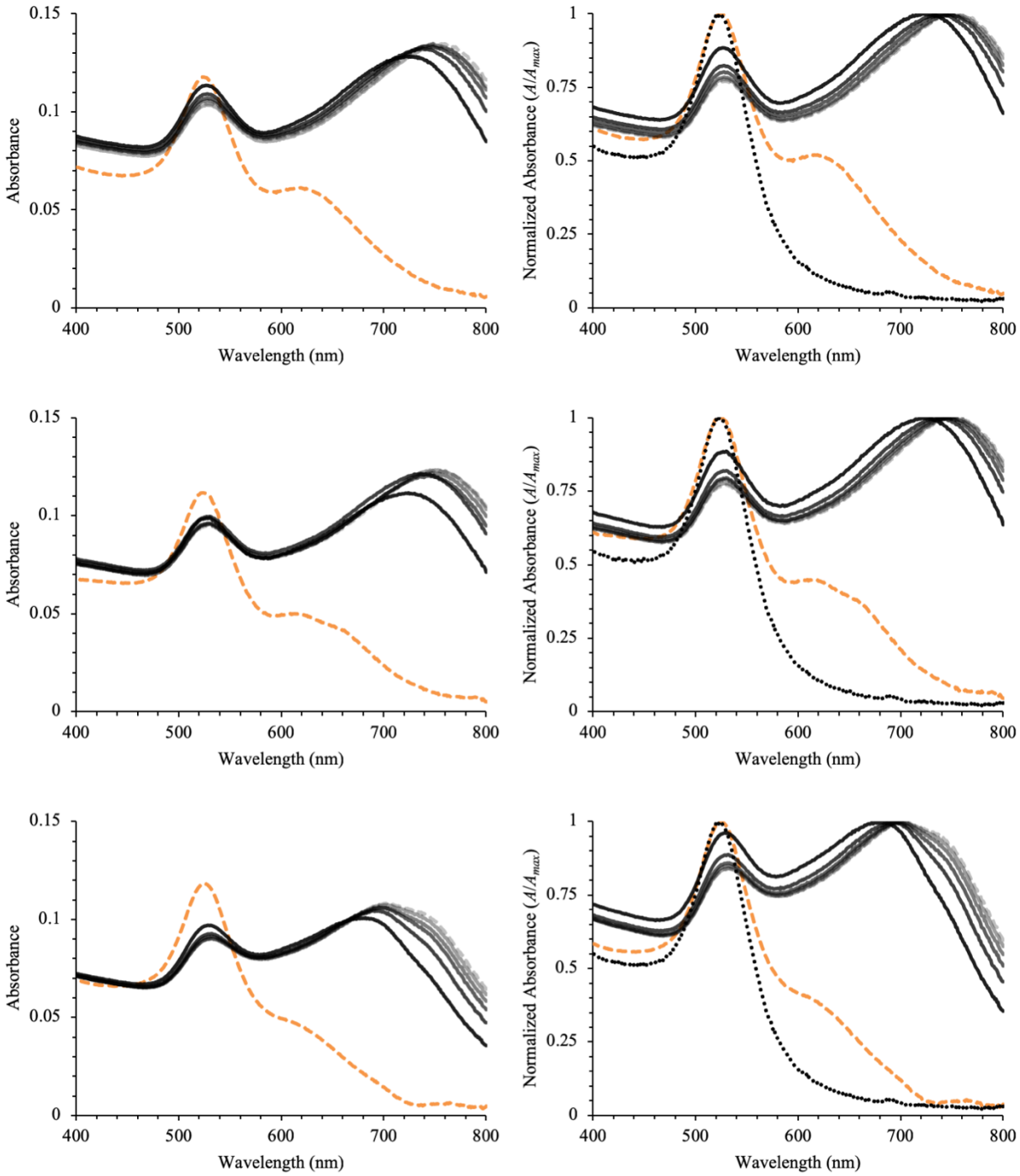

Figure S13. (Left) Background-corrected and (right) background-corrected and normalized (A/A_{max}) UV-Vis spectra for PEG-AuNPs in nitrification wastewater matrix. Orange dashed-line depicts UV-Vis spectra at $t \approx 0$ minutes, grey dashed-line depicts spectra at $t = 120$ minutes, and grey-scale depicts spectra at 20-minutes intervals in between (black-to-grey). For reference, the black dotted-line depicts the UV-Vis spectra in DDI.

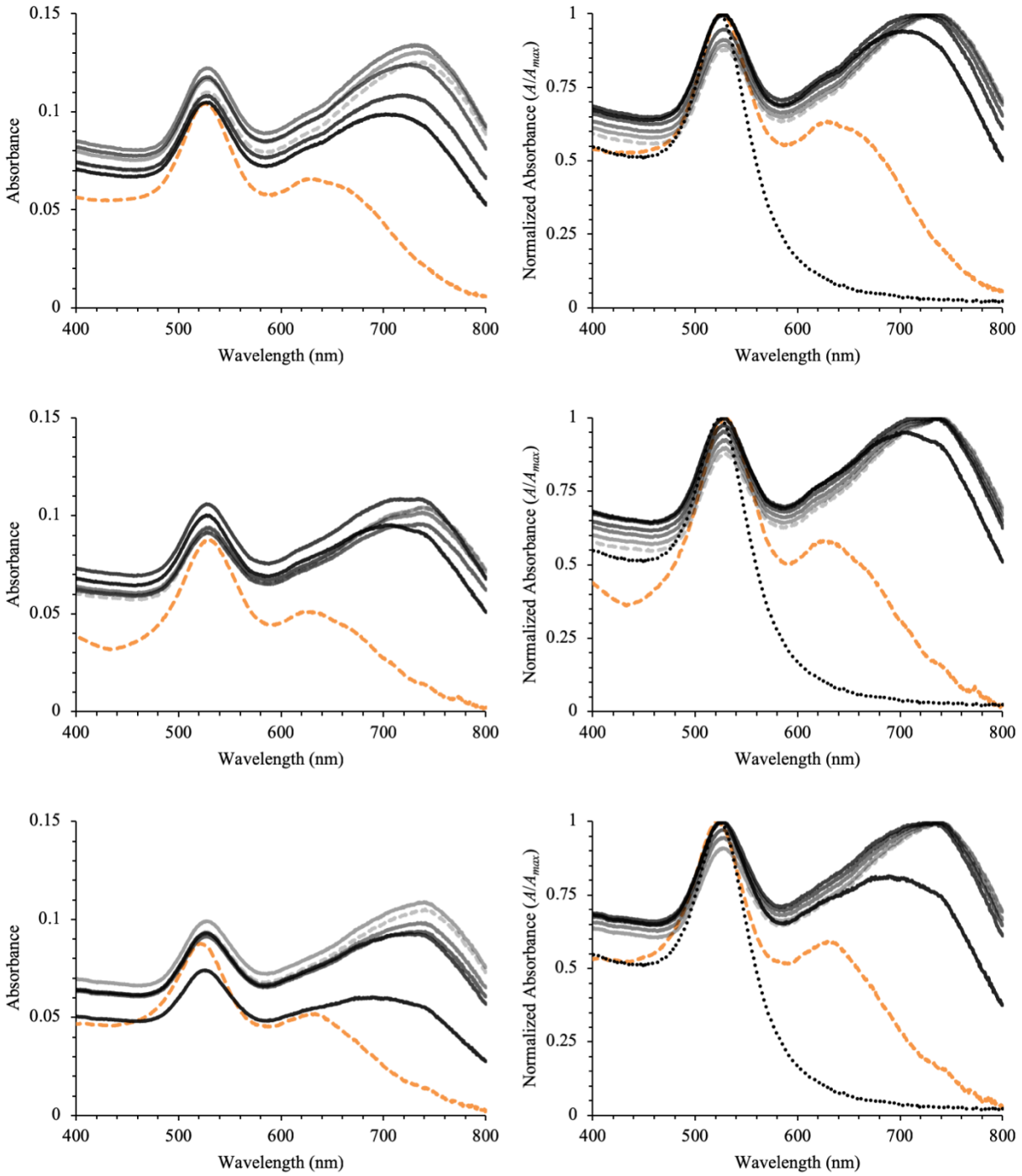

Figure S14. (Left) Background-corrected and (right) background-corrected and normalized (A/A_{max}) UV-Vis spectra for COOH-AuNPs in influent wastewater matrix. Orange dashed-line depicts UV-Vis spectra at $t \approx 0$ minutes, grey dashed-line depicts spectra at $t = 120$ minutes, and grey-scale depicts spectra at 20-minutes intervals in between (black-to-grey). For reference, the black dotted-line depicts the UV-Vis spectra in DDI.

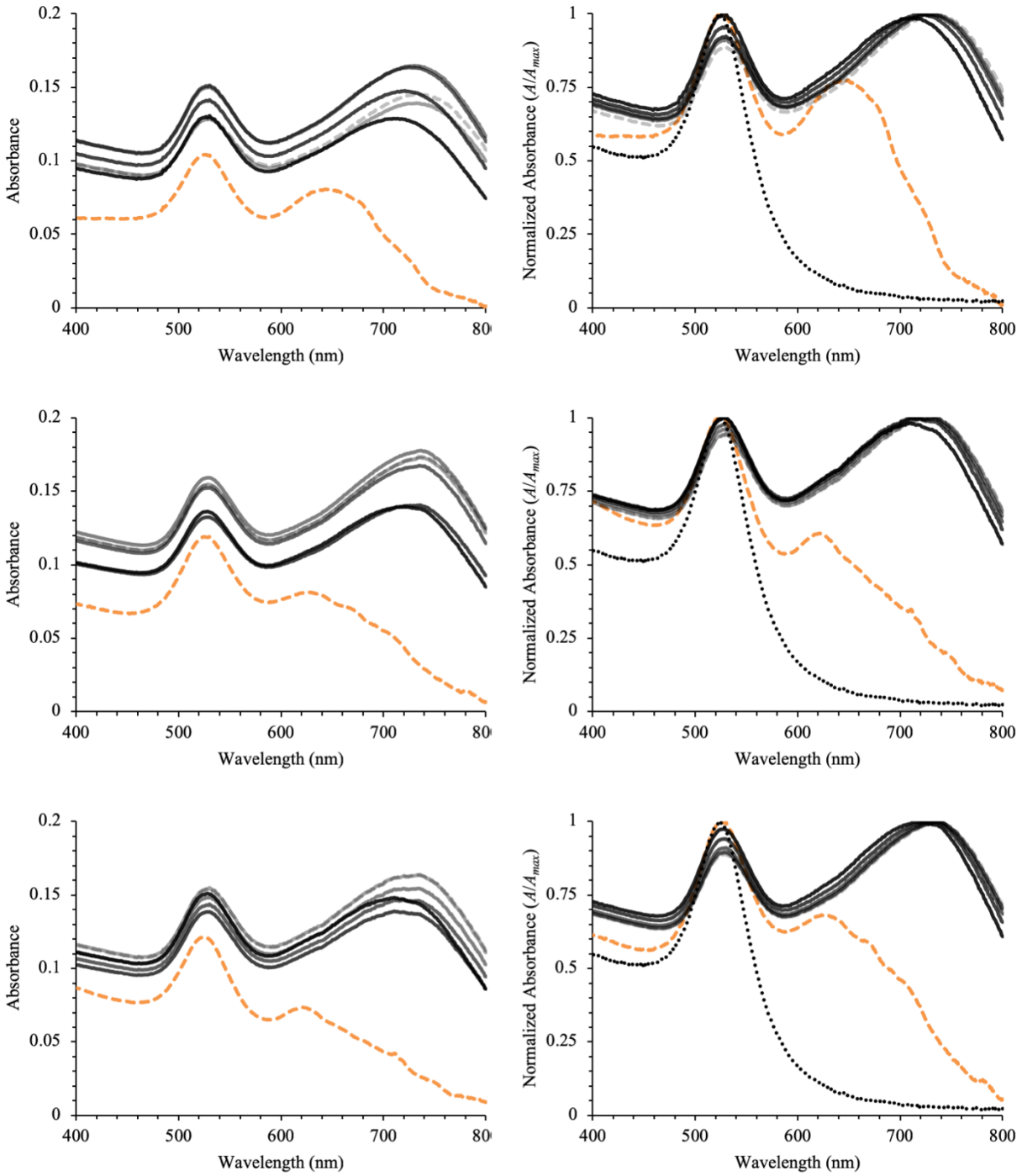

Figure S15. (Left) Background-corrected and (right) background-corrected and normalized (A/A_{max}) UV-Vis spectra for COOH-AuNPs in denitrification wastewater matrix. Orange dashed-line depicts UV-Vis spectra at $t \approx 0$ minutes, grey dashed-line depicts spectra at $t = 120$ minutes, and grey-scale depicts spectra at 20-minutes intervals in between (black-to-grey). For reference, the black dotted-line depicts the UV-Vis spectra in DDI.

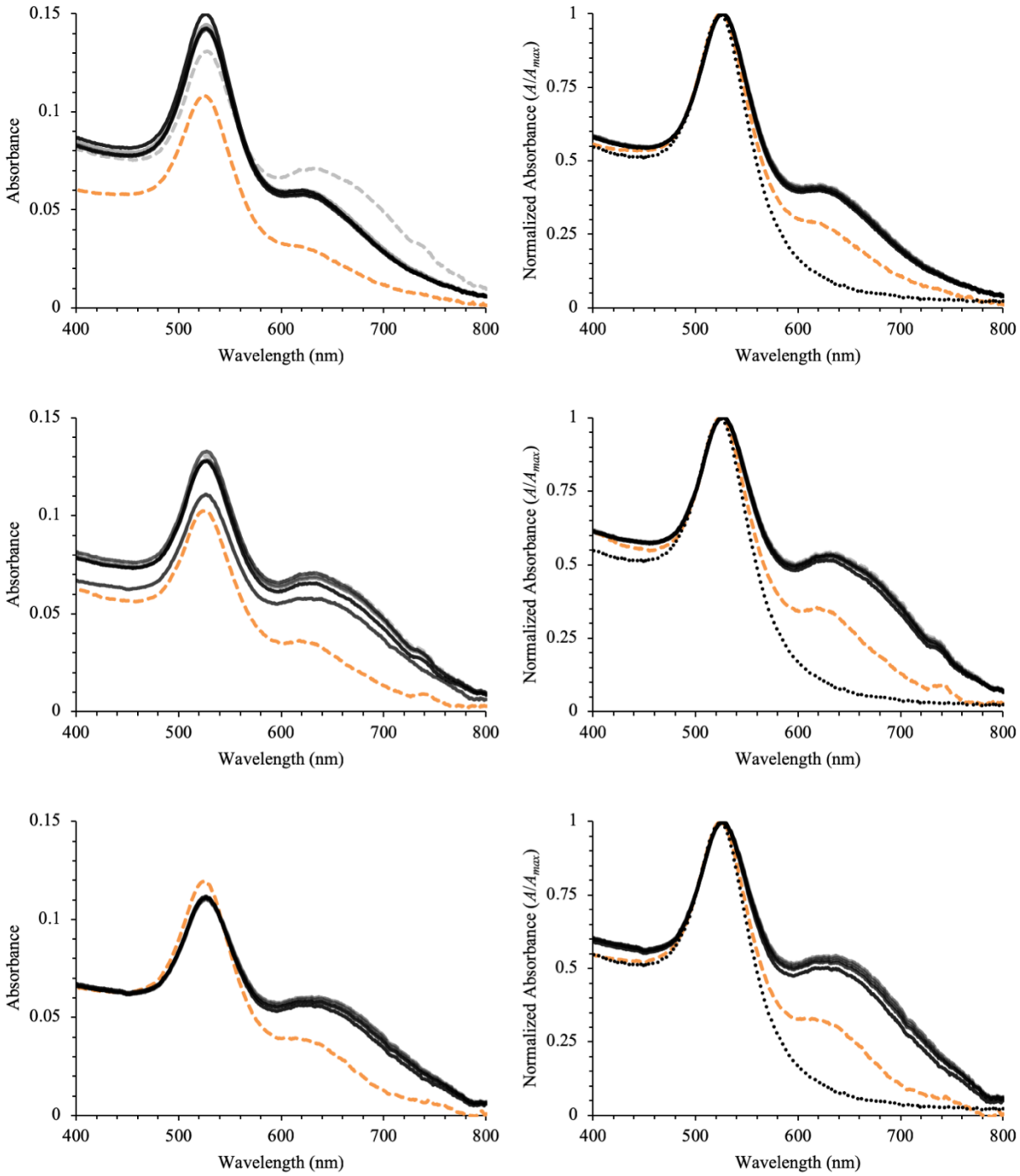

Figure S16. (Left) Background-corrected and (right) background-corrected and normalized (A/A_{max}) UV-Vis spectra for COOH-AuNPs in nitrification wastewater matrix. Orange dashed-line depicts UV-Vis spectra at $t \approx 0$ minutes, grey dashed-line depicts spectra at $t = 120$ minutes, and grey-scale depicts spectra at 20-minutes intervals in between (black-to-grey). For reference, the black dotted-line depicts the UV-Vis spectra in DDI.

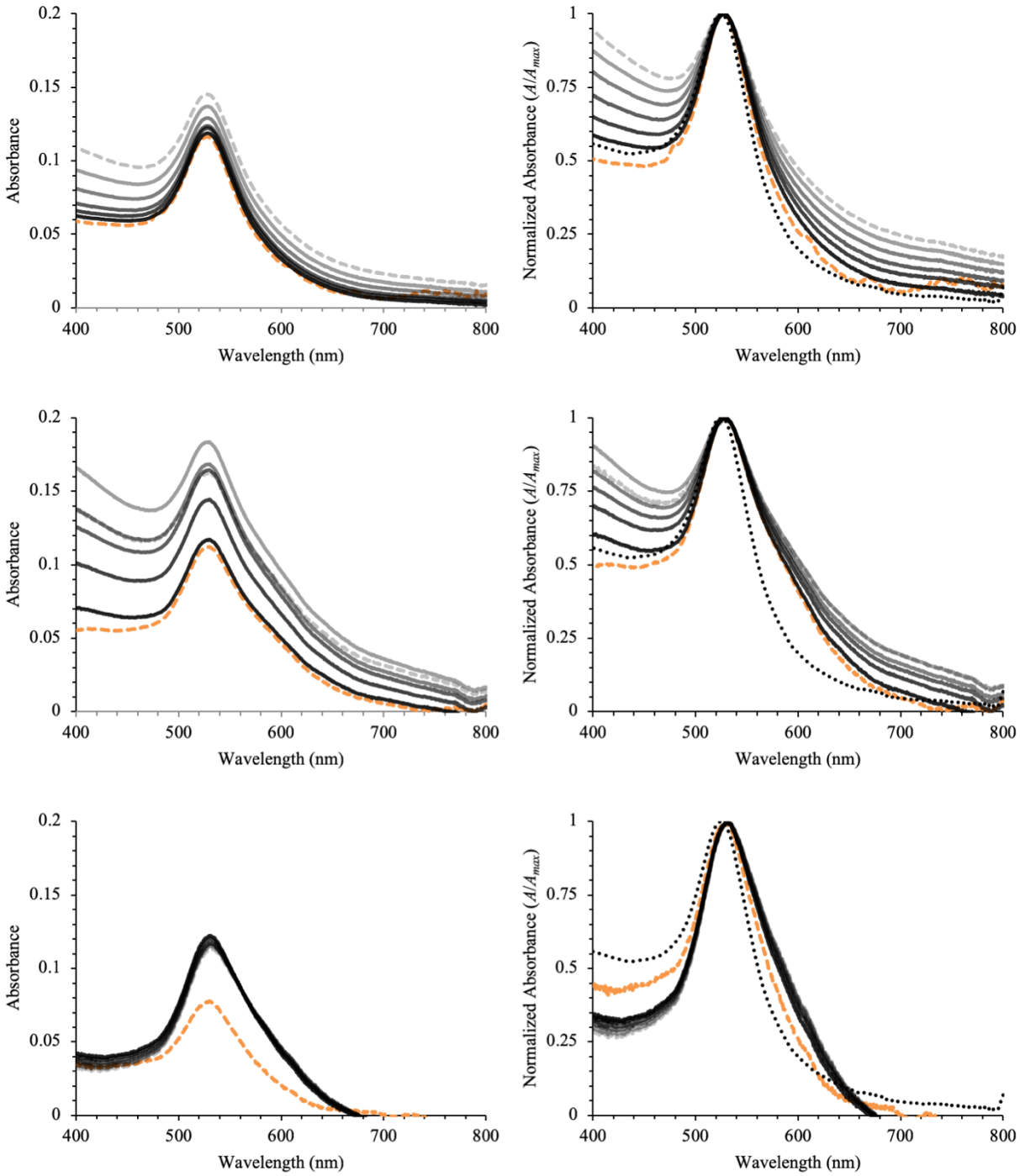

Figure S17. (Left) Background-corrected and (right) background-corrected and normalized (A/A_{max}) UV-Vis spectra for bPEI-AuNPs in influent wastewater matrix. Orange dashed-line depicts UV-Vis spectra at $t \approx 0$ minutes, grey dashed-line depicts spectra at $t = 120$ minutes, and grey-scale depicts spectra at 20-minutes intervals in between (black-to-grey). For reference, the black dotted-line depicts the UV-Vis spectra in DDI.

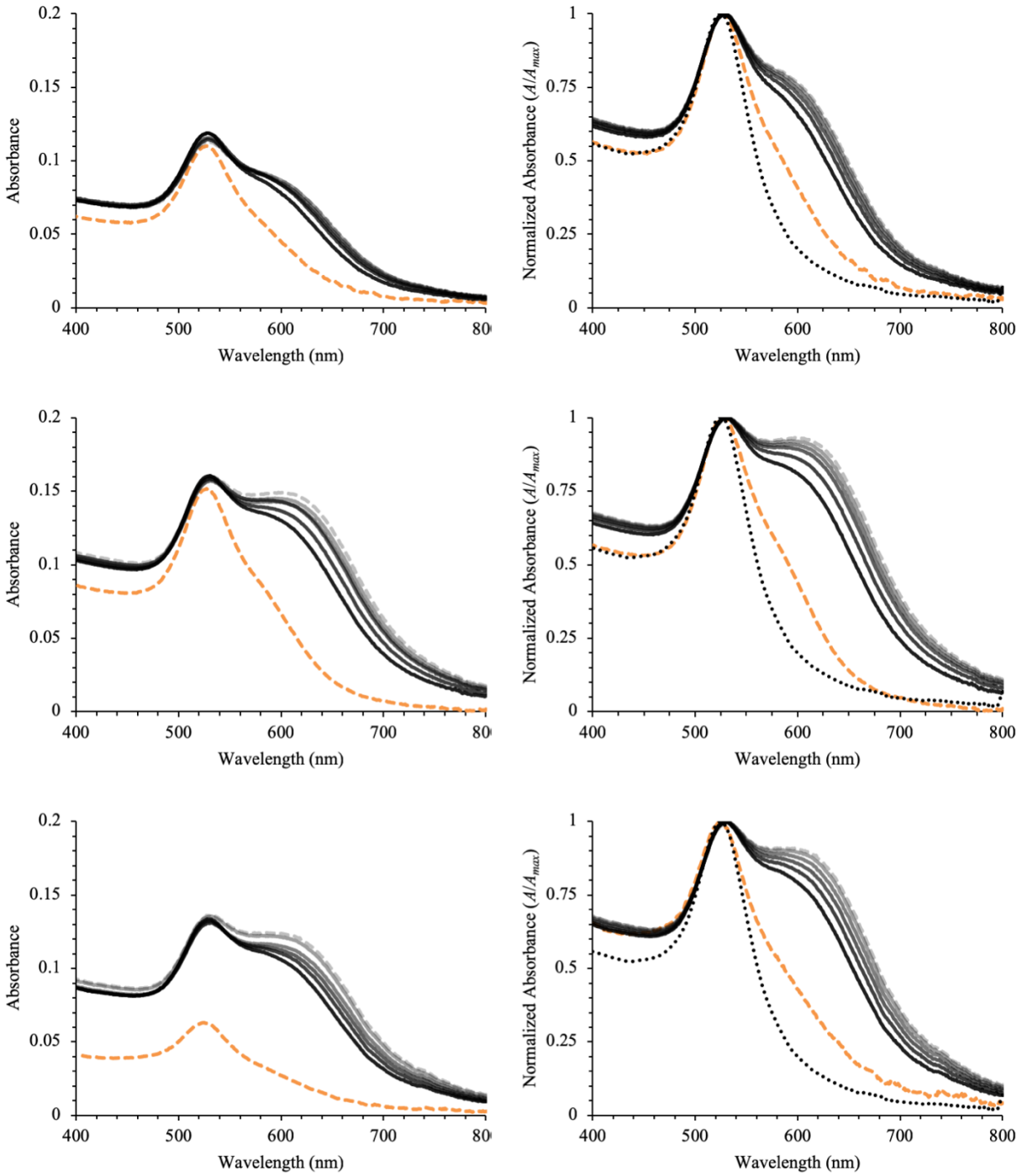

Figure S18. (Left) Background-corrected and (right) background-corrected and normalized (A/A_{max}) UV-Vis spectra for bPEI-AuNPs in denitrification wastewater matrix. Orange dashed-line depicts UV-Vis spectra at $t \approx 0$ minutes, grey dashed-line depicts spectra at $t = 120$ minutes, and grey-scale depicts spectra at 20-minutes intervals in between (black-to-grey). For reference, the black dotted-line depicts the UV-Vis spectra in DDI.

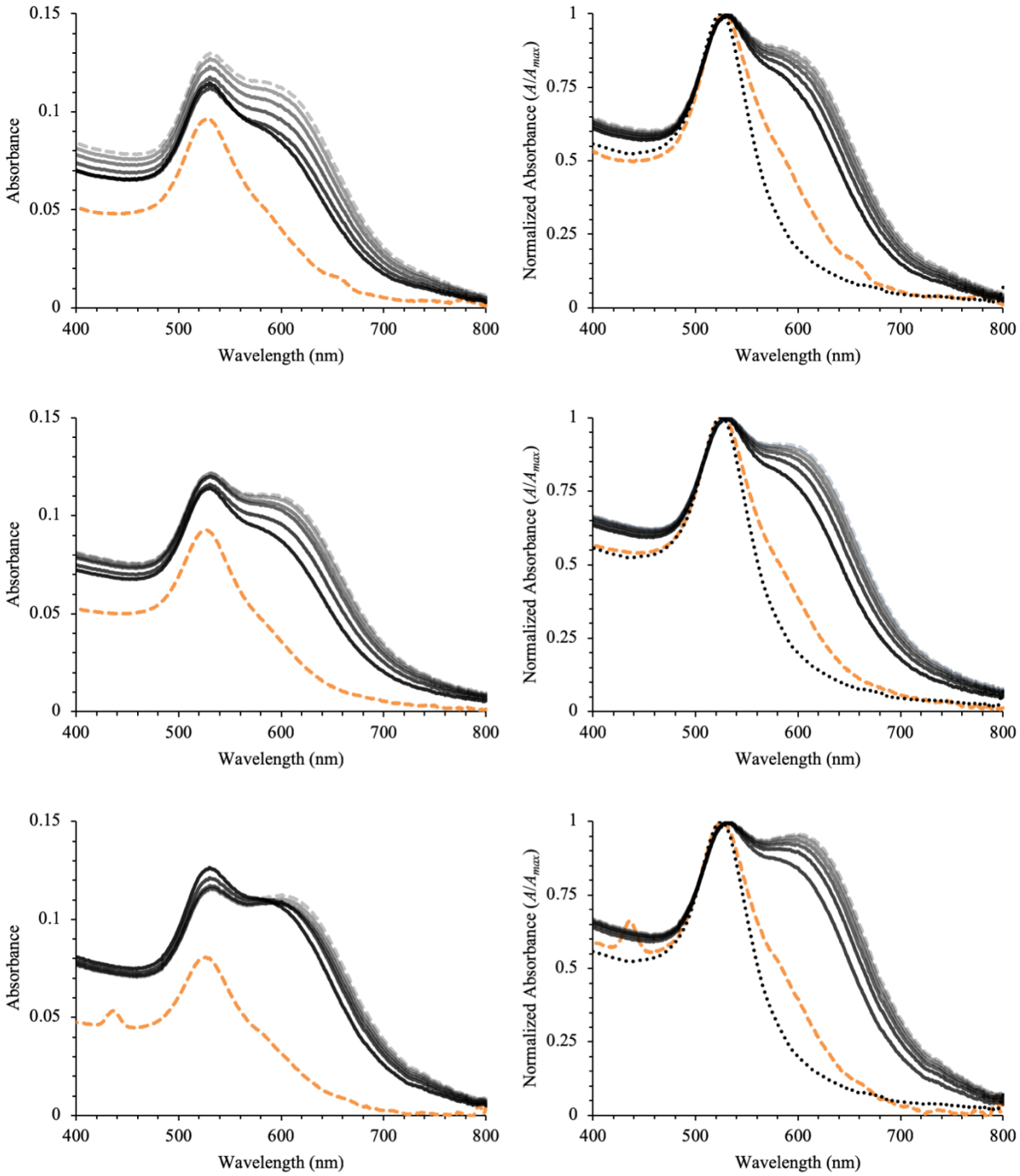

Figure S19. (Left) Background-corrected and (right) background-corrected and normalized (A/A_{max}) UV-Vis spectra for bPEI-AuNPs in nitrification wastewater matrix. Orange dashed-line depicts UV-Vis spectra at $t \approx 0$ minutes, grey dashed-line depicts spectra at $t = 120$ minutes, and grey-scale depicts spectra at 20-minutes intervals in between (black-to-grey). For reference, the black dotted-line depicts the UV-Vis spectra in DDI.

Transmission Electron Microscopy Micrographs – Interparticle Distance Analysis

The transmission electron microscope (TEM) images were used to determine the average center-to-center separation distance (d_s) between neighboring particles. The average ratio between d_s and the nanoparticle diameter was then calculated for each AuNP type after incubating in a given wastewater matrix. To accomplish this, a typical TEM micrograph was analyzed using the software package Fiji (ImageJ)[6,7] and the ParticleSizer v1.07 plugin[8] according to the following procedure.

1. The centroid of each AuNP primary particle was identified by delineating each primary particle using the default settings of the ParticleSizer plugin[8], except that the minimal ferret length and the minimum long and short ellipsis axes were each set to 3 pixels. These values were found to correctly delineate the AuNPs while minimizing the inclusion of non-AuNP particles (i.e., false-positives) and 'lumping' of adjacent primary particles.
2. Using the x- and y-coordinate of the centroid, the Euclidean center-to-center separation distance (d_s) between each pair of primary particles was calculated. To eliminate particle pairs that were either not adjacent or were overlapping (i.e., the primary particles were vertically stacked on top of each other, an artifact from analyzing a 3-D sample in 2-D), these distances were constrained by the lower- and upper-bounds shown in Table S4. These limits correspond to the average AuNP core diameter measured via TEM minus its lower 95% confidence interval and the hydrodynamic diameter measured via DLS plus its upper 95% confidence interval, respectively (Table 1). Based on an analysis without these constraints, the range in d_s were found to span ≈30 nm to >1,000 nm, with high values in d_s clearly indicating primary particle pairs that were not adjacent to each other.
3. The values of d_s retained after applying the bounds in Table S4 were then compiled and the distribution of the values and accompanying statistics were generated.

An illustrative example of these steps is shown in Figure S20, with the full results from this analysis shown in Figures S21 – S23.

Table S4. Lower- and upper-bounds applied to each AuNP type during TEM analysis.

Surface Coating	Lower Bound (d_c – Lower 95% C.I) (nm)	Upper Bound (D_h + Upper 95% C.I) (nm)
PEG	37	49.3
COOH	35	52.2
bPEI	37	52.9

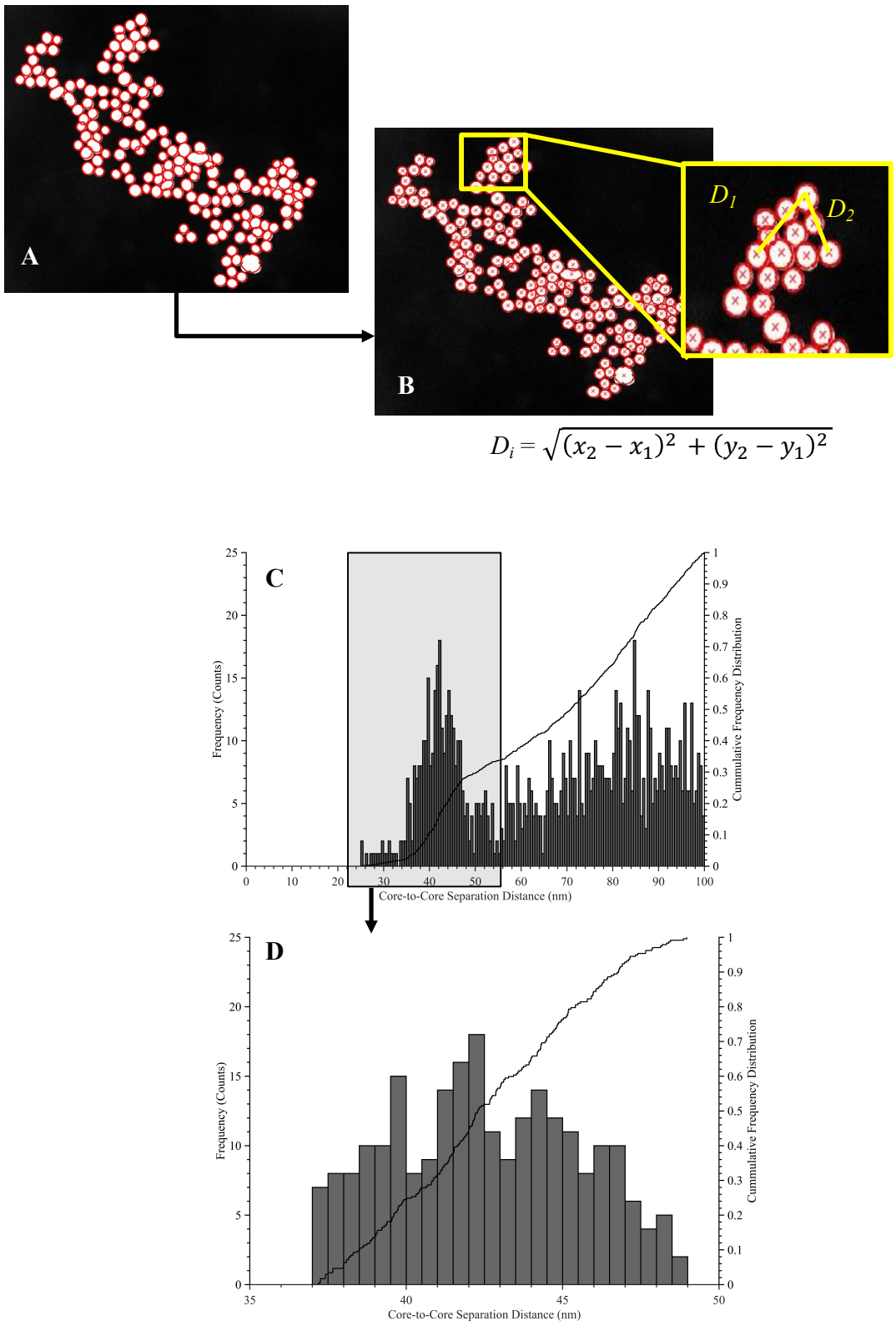

Figure S20. Illustrative example of center-to-center separation distances (d_s) calculated for PEG-AuNPs incubated in influent wastewater matrix: (a) delineation of primary particles and (b) identification of particle centroids (Steps 1 and 2); (c) distribution of d_s without constraints; and (d) distribution of d_s with constraints.

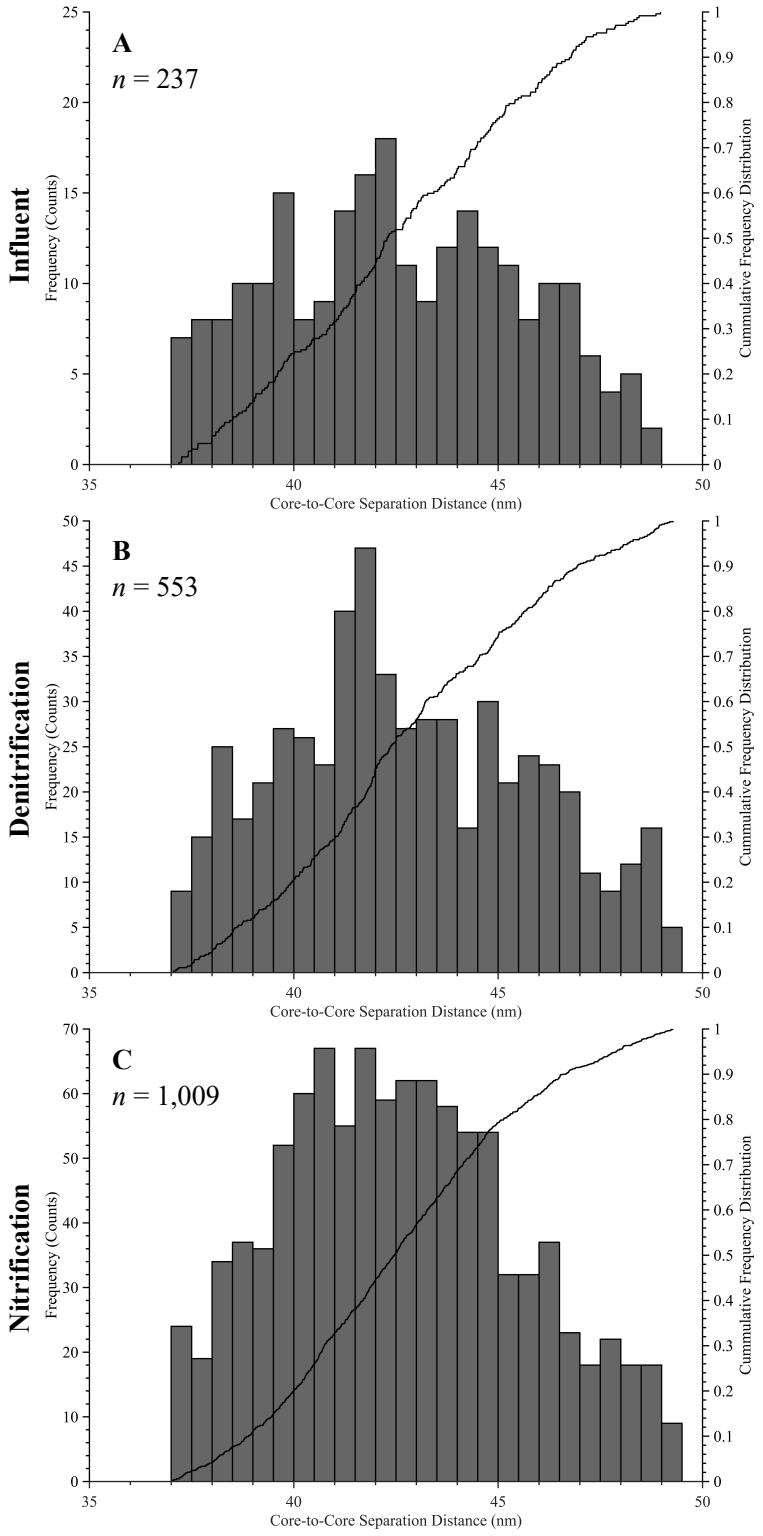

Figure S21. Distribution of center-to-center separation distances (d_s) calculated for PEG-AuNPs incubated in (a) influent, (b) denitrification, and (c) nitrification wastewater matrices after t = 120 minutes.

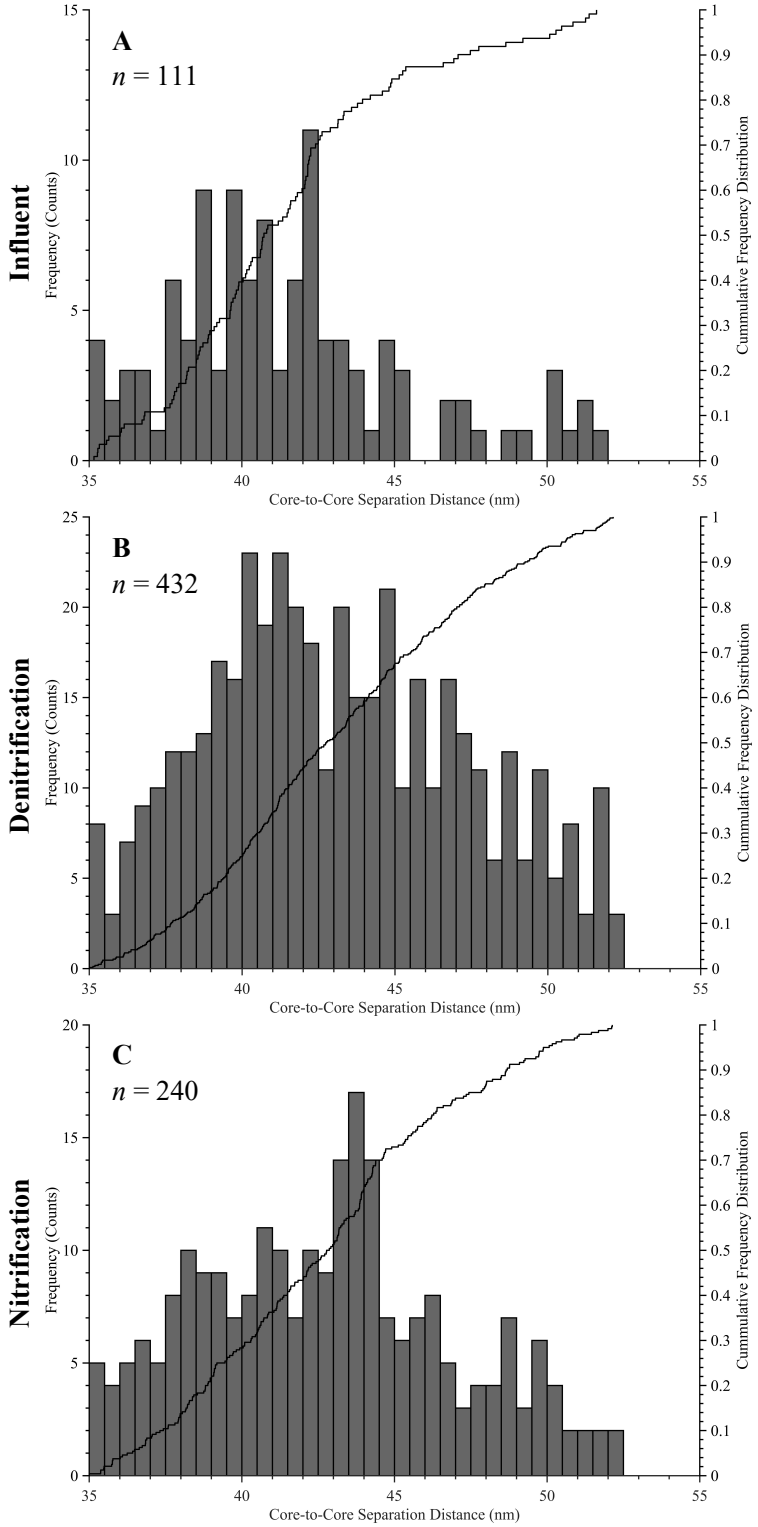

Figure S22. Distribution of center-to-center separation distances (d_s) calculated for COOH-AuNPs incubated in (a) influent, (b) denitrification, and (c) nitrification wastewater matrices after t = 120 minutes.

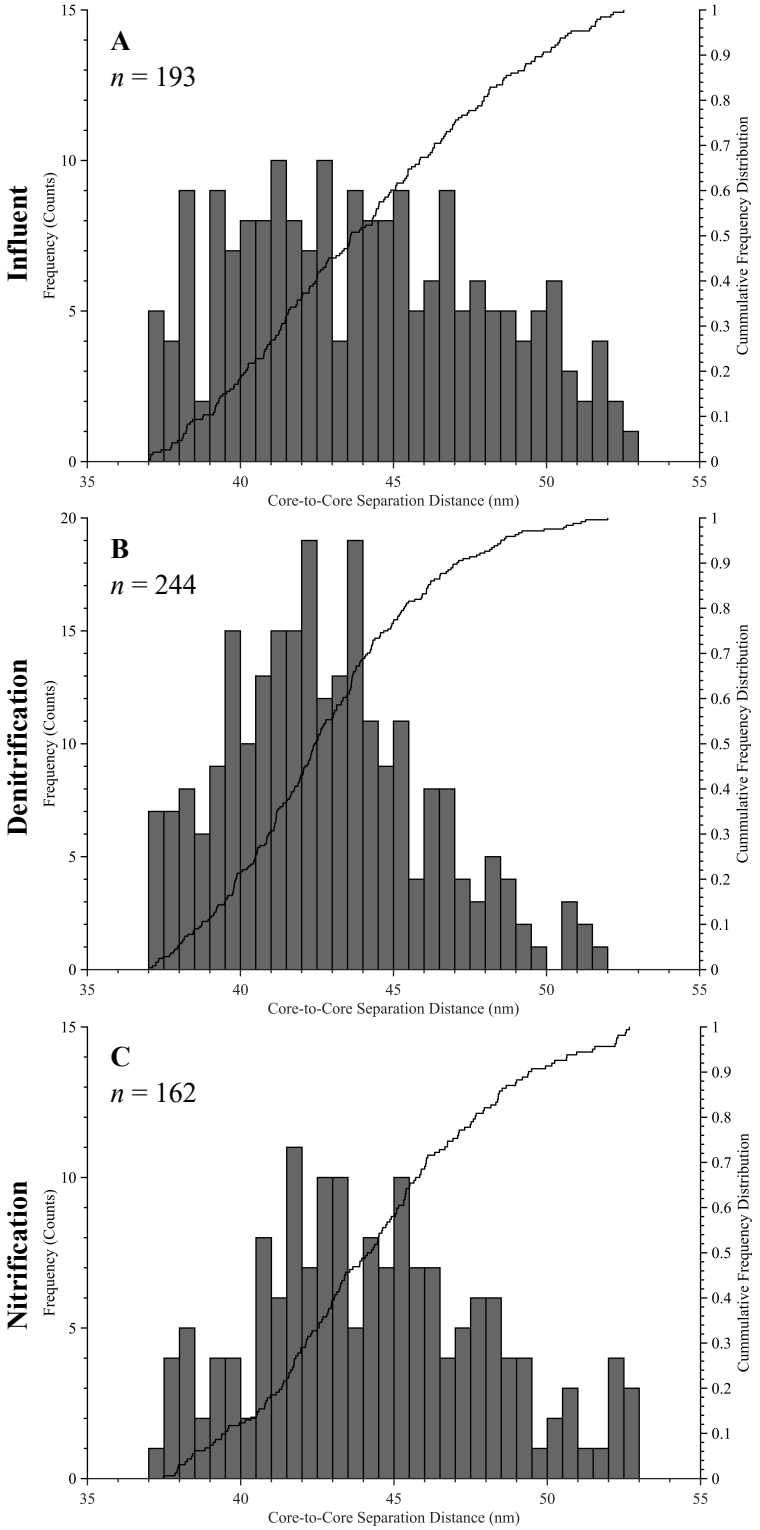

Figure S23. Distribution of center-to-center separation distances (d_s) calculated for bPEI-AuNPs incubated in (a) influent, (b) denitrification, and (c) nitrification wastewater matrices after t = 120 minutes.

Transmission Electron Microscopy Micrographs – Matrix Exchange

Examples of the micrographs collected via transmission electron microscopy (TEM) after the AuNPs had gone through the double matrix exchange procedure via TFF are shown in Figure S24. The samples were prepared according to the procedures described in the main text.

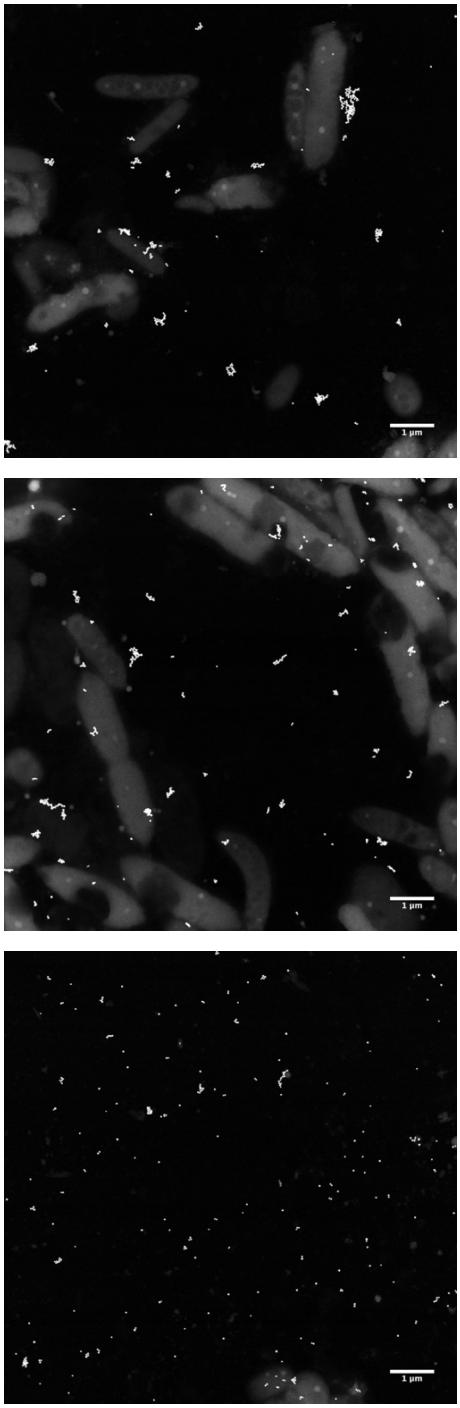

Figure S24. TEM-HAADF micrograph of (top) PEG-, (middle) COOH-, and (bottom) bPEI-AuNPs after incubating for ≈240 minutes during the double matrix exchange procedure.

References

(1) Henry, D. C. The cataphoresis of suspended particles. Part I. – The equation of cataphoresis. *Proc. Roy. Soc. A* **1931**, *133* (821), 106.

(2) Ohshima, H. A simple expression for Henry's function for the retardation effect in electrophoresis of spherical colloidal particles. *J. Colloid Interface Sci.* **1994**, *11* (1), 269 – 271.

(3) Hunter, R.J. *Foundations of Colloid Science*, *2nd Edition* **2002**. Oxford University Press, London, United Kingdom.

(4) Benjamin, M. M.; Lawler, D.F. *Water Quality Engineering – Physical/Chemical Treatment Processes* **2013**. John Wily & Sons, Inc., Hoboken, New Jersey.

(5) American Water Works Association (AWWA) *Standard Methods for the Examination of Water and Wastewater, 22nd Edition* **2012**. American Public Health Association.

(6) C. A. Schneider, W. S. Rasband and K. W. Eliceiri, NIH Image to ImageJ: 25 years of image analysis, *Nat. Methods*, **2012**, 9, 671–675.

(7) J. Schindelin, I. Arganda-Carreras, E. Frise, V. Kaynig, M. Longair, T. Pietzsch, S. Preibisch, C. Rueden, S. Saalfeld, B. Schmid, J.-Y. Tinevez, D. J. White, V. Hartenstein, K. Eliceiri, P. Tomancak and A. Cardona, Fiji: an open-source platform for biological-image analysis, *Nat. Methods*, **2012**, 9, 676–682.

(8) Wagner, T., ij-particlesizer: ParticleSizer 1.0.7 Zendo 10.5281/zenodo.56457, **2017**.